

# Reverse Engineering a Multivariable Controller: A Case Study

J. S. Freudenberg and A. Y. Karnik

**Abstract**—In this paper, we consider a case study for which multivariable control achieves better performance than decentralized control due to plant interactions and bandwidth limitations. We analyze the structure of the multivariable controller by introducing an “equivalent controller” that achieves the same performance, but is more amenable to simplification. We then show analytically that the multivariable controller must necessarily have the structure of the one that was designed.

## I. INTRODUCTION

The use of decentralized feedback loops for multiple input multiple output (MIMO) systems is desirable from an economic standpoint. However, as described in [1], a decentralized control architecture may result in performance limitations and tradeoffs. The use of a multivariable controller may alleviate some of these, albeit at the cost of additional controller complexity. Since the plant limitations are unchanged by the introduction of a more complex controller structure, it is interesting to determine how a multivariable controller that achieves improved performance does so. Such an understanding may yield insight into how the controller may be simplified and implemented. Such an analysis of controller architecture has appeared in the automotive literature [7].

The case study in the present paper is the design of a MIMO controller for a Reactive Ion Etcher (RIE), a plasma based processing tool used in the manufacture of integrated circuits [2]–[5]. The performance is measured by the ability of the feedback system to track step commands without excessive actuator activity. It was found in [1] that a decentralized controller implemented for this system has the property that performance in one loop deteriorates as that of the other loop is improved. A multivariable controller designed using LQG techniques yields improved performance, but is considerably more complex than a low order decentralized controller. This motivates an attempt to simplify the multivariable controller by understanding how it works. Indeed, if a first principles understanding of the controller is available, then such a simplified controller may be designed at the outset.

J. S. Freudenberg is with Department of Electrical Engineering and Computer Science, University of Michigan, Beal Avenue, Ann Arbor, MI 48109-2122, USA jfr@umich.edu

A.Y. Karnik is with Department of Mechanical Engineering, University of Michigan, 2350 Hayward St., Ann Arbor, MI 48109-2125 USA akarnik@umich.edu

## II. DESIGN CRITERIA AND INITIAL CONTROLLER DESIGNS

The model used in the design study [2] was

$$\begin{bmatrix} [F] \\ V_{bias} \end{bmatrix} = P \begin{bmatrix} Power \\ Throttle \end{bmatrix}, \quad (1)$$

where the  $(i, j)$ 'th element of  $P$  is denoted by  $p_{ij}$ . The plant outputs are  $[F]$ , the concentration of fluorine in the plasma, and  $V_{bias}$ , the DC self bias voltage between the powered and grounded electrodes. The inputs are the angle of the throttle for the cryo pump used to remove gasses from the chamber, and the RF power supplied to the reactor. The primary design considerations [1] were: First, the controller should track step commands to  $V_{bias}$  and  $[F]$  with zero steady state error; this necessitates the use of integral control. Second, the throttle actuator is quite nonlinear, thus requiring that overshoot in the throttle response to  $V_{bias}$  and  $[F]$  step commands be limited to less than 5%.

To facilitate controller design and analysis, the plant inputs and outputs were scaled by their nominal values, yielding transfer functions

$$P(s) = \begin{bmatrix} \frac{5.67s+23.3}{s^2+15s+26.7} & \frac{-0.071e^{-0.5s}}{s+0.24} \\ \frac{0.8}{s+0.97} & \frac{(0.086s+0.35)e^{-0.5s}}{s^2+4s+0.7} \end{bmatrix}. \quad (2)$$

Bode plots of the scaled plant are depicted in Figure 1. Note that Power has higher bandwidth than throttle, and affects  $[F]$  and  $V_{bias}$  approximately identically at low to mid frequencies. Since  $[F]$  is considered a more critical

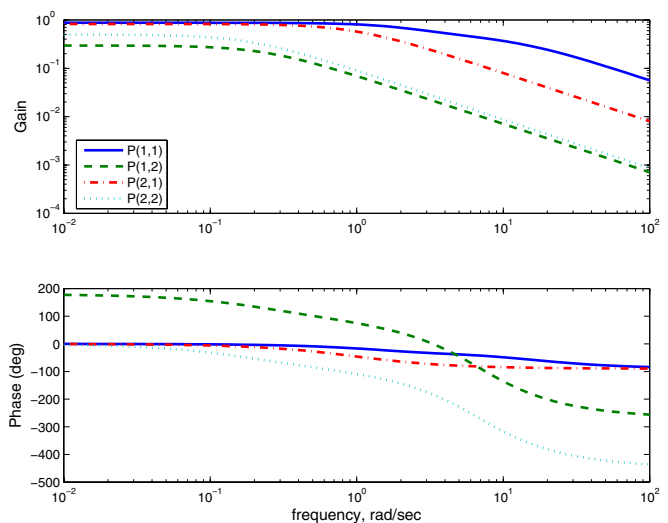


Fig. 1. Bode Plots of the Scaled Plant.

process variable, Power is used to track  $[F]$ . This leaves Throttle to be used to track  $V_{bias}$ . The Power- $[F]$  loop may thus have higher bandwidth than the Throttle- $V_{bias}$  loop, because the bandwidth limitation in the latter loop is more severe due to limited actuator authority.

Consider the decentralized controller

$$C(s) = \begin{bmatrix} \frac{2s+0.5}{s^3+2.25s^2+1.25s} & 0 \\ 0 & \frac{0.4(3s+0.21)}{s^2+s} \end{bmatrix}. \quad (3)$$

The responses of the plant inputs and outputs to step commands are given in Figure 2. Note the rather sluggish

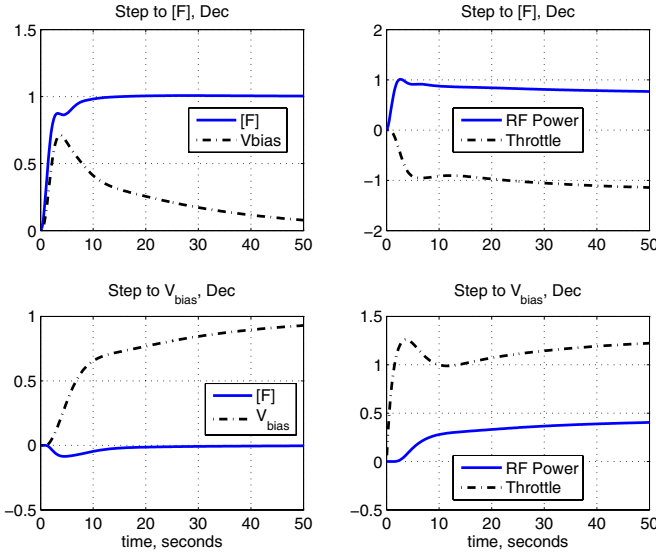


Fig. 2. Step Responses for the Decentralized Controller (3).

response of  $V_{bias}$ . It was found that increasing the bandwidth of the  $V_{bias}$  loop allowed the  $V_{bias}$  error due to a step in  $[F]$  to be driven more rapidly to zero at the expense of increased throttle activity. On the other hand, decreasing the bandwidth of the  $[F]$  loop resulted in a smaller disturbance to  $V_{bias}$  due to a step in  $[F]$  at the expense of slower  $[F]$  command tracking.

Refer to the decentralized control architecture in Figure 3, and suppose we first close the Power to  $[F]$  loop.

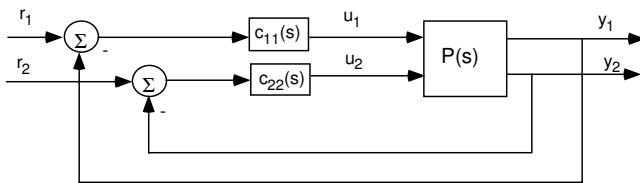


Fig. 3. Decentralized Control.

The resulting scalar feedback loop will have a sensitivity function given by  $s_1 = 1/(1+p_{11}c_{11})$ . Suppose next that the second loop is closed, and denote the multivariable output sensitivity function by  $S_O = (I + PC)^{-1}$ . Here, let  $S_{Oij}$  represent the individual elements of  $S_O$ . Then the response

of the throttle control input to a step in  $V_{bias}$  is given by  $c_{22}S_{O22}$ . Finally, suppose that the first loop is closed so that

$$|s_1(j\omega)| < \epsilon_1(\omega), \quad (4)$$

and that the second loop is closed so that

$$|c_{22}(j\omega)S_{O22}(j\omega)| < \epsilon_2(\omega). \quad (5)$$

If both  $\epsilon_1(j\omega) \ll 1$  and  $\epsilon_2(j\omega) \ll 1$ , then it is shown in [1] that

$$|S_{O21}(j\omega)| \approx |p_{21}(j\omega)|/|p_{11}(j\omega)|. \quad (6)$$

Suppose that high bandwidth is used in the first loop to achieve good tracking of  $[F]$  commands, and that low bandwidth is used in the second loop to prevent excessive throttle response. Then necessarily a large closed loop interaction will exist at any frequency for which the ratio (6) is not sufficiently small.

A multivariable LQG controller with augmented integrators is depicted in Figure 4. Suppose that the state feedback

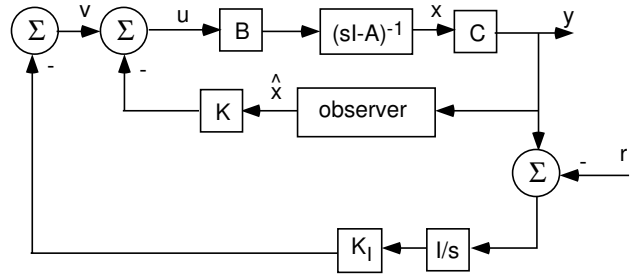


Fig. 4. Observer Based Compensator with Integral Control.

and observer gains are chosen by setting the state cost to

$$Q = \begin{bmatrix} C^T Q_1 C & 0 \\ 0 & Q_I \end{bmatrix}, \quad Q_1 = \begin{bmatrix} 10 & 0 \\ 0 & 12 \end{bmatrix}, \quad Q_I = \begin{bmatrix} 0.48 & 0 \\ 0 & 0.54 \end{bmatrix},$$

the control cost to  $R = I$ , and the process and measurement noise intensities to  $V = 9BB^T$  and  $W = I$ . The step response of the closed loop system, depicted in Figure 5, shows that use of this multivariable controller allows more flexibility to make the tradeoff between (i) the speed of response to a  $[F]$  command, (ii) overshoot in the throttle response, and (iii) size of the closed loop interactions. In the next section we analyze this controller to see how these improvements were achieved.

### III. EQUIVALENT CONTROLLER ANALYSIS

The relative performance of the decentralized and multivariable controllers was evaluated solely on the basis of the command response, and hence is unaffected by the observer. Indeed, it is easy to verify that the command response is given by the transfer function

$$T_{yr}(s) = (I + P(s)(I + K(sI - A)^{-1}B)^{-1}K_I/s)^{-1} P(s)(I + K(sI - A)^{-1}B)^{-1}K_I/s. \quad (7)$$

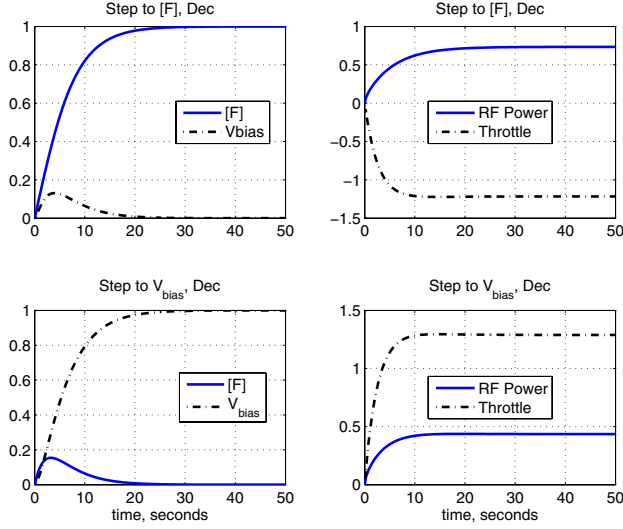


Fig. 5. Target Step Responses with Multivariable Controller

To facilitate analysis of the multivariable controller, it is convenient to rearrange the system in Figure 4 into the form shown in Figure 6, where  $C_{eq}$  is chosen to achieve a

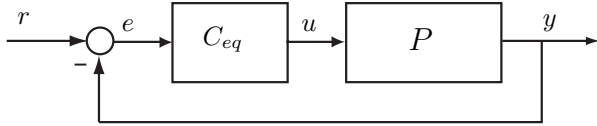


Fig. 6. Unity Feedback Compensator with Command Response Equivalent to that of Figure 4.

command response equivalent to that of the observer based compensator:

$$C_{eq}(s) = (I + K(sI - A)^{-1}B)^{-1}K_I/s. \quad (8)$$

It is easy to verify that the output complementary sensitivity function,  $T_O = (I + PC_{eq})^{-1}PC_{eq}$ , of the system shown in Figure 6 is identical to (7). Hence the command response of the two systems is equivalent. Note that all plant poles appear as zeros of  $C_{eq}$ , and thus the rearrangement depicted in Figure 6 is applicable only to stable plants. It will also be undesirable to use  $C_{eq}$  for a plant with lightly damped poles.

Bode plots of the elements of  $C_{eq}$  are depicted in Figure 7, and show that the (1,1) and (1,2) elements of  $C_{eq}$  are approximately identical and that each have the form of an integrator augmented with additional phase lead. Similarly, the (2,1) and (2,2) elements of  $C_{eq}$  are approximately equal in magnitude and opposite in sign, and also have the form of integrators with additional phase lead. This observation motivates us to consider a lower order approximation to  $C_{eq}$ ,

$$\hat{C}_{eq} = \begin{bmatrix} C_{d1} & 0 \\ 0 & C_{d2} \end{bmatrix} \begin{bmatrix} 1 & 1 \\ -1 & 1 \end{bmatrix}, \quad (9)$$

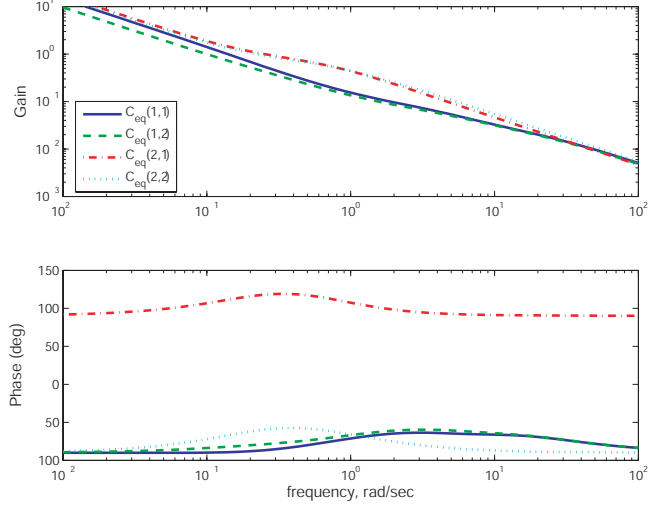


Fig. 7. Bode Plots of Equivalent Compensator.

where  $C_{d1}$  and  $C_{d2}$  are given by

$$C_{d1} = 0.29(s+1)(s+2.1)/(s(s+1.27)(s+3.8))$$

$$C_{d2} = 0.57(s+0.18)/(s(s+0.65)).$$

Comparisons of the Bode plots of the diagonal elements of  $C_{eq}$  and  $\hat{C}_{eq}$  in Figure 8 and the step responses in Figure 9 show that the lower order approximations yield approximately the same performance.

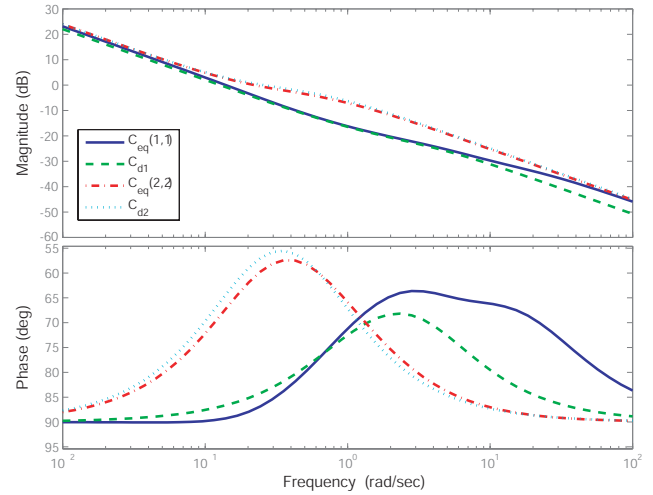


Fig. 8. Bode Plots of Diagonal Elements of  $C_{eq}$  and Approximations  $C_{d1}$  and  $C_{d2}$ .

The preceding analysis suggests that the multivariable controller uses the higher authority RF power actuator to control the *average* of  $[F]$  and  $V_{bias}$ , and the lower authority throttle actuator to control the *difference* between  $[F]$  and  $V_{bias}$ . This can be justified from the Bode plots of the plant in Figure 1, which show that Power has roughly equal authority over  $[F]$  and  $V_{bias}$  at frequencies below 1 rad/sec, and thus little authority over the difference  $[F] - V_{bias}$ .

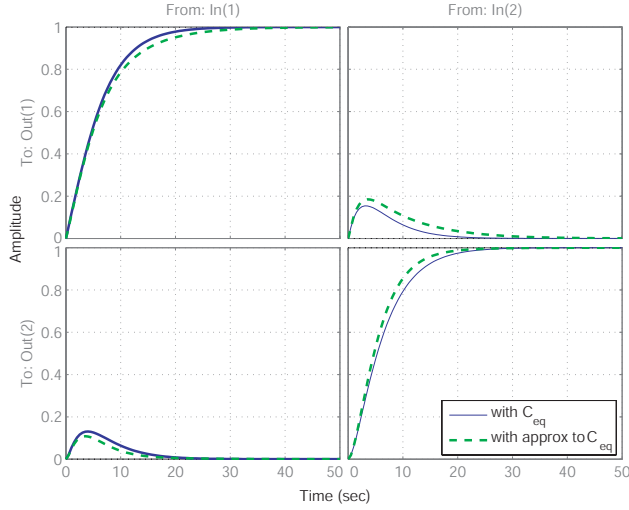


Fig. 9. Step Response with  $C_{eq}$  and  $\hat{C}_{eq}$ .

By way of contrast, consider the decentralized architecture of Figure 3, and suppose that Power is used to control one of these two outputs (say  $[F]$ ). Then the control signal used to regulate  $[F]$  to a desired value will act as a disturbance to  $V_{bias}$  that cannot be attenuated rapidly because  $V_{bias}$  is regulated by the throttle, which has relatively low authority at high frequencies. Conversely, were RF power used to regulate  $V_{bias}$ , a command to  $V_{bias}$  would cause a disturbance to  $[F]$ . Hence, by allowing the Power control signal to depend upon tracking errors in both  $[F]$  and  $V_{bias}$ , the multivariable controller achieves a compromise between these two outputs: although the ability of the controller to drive  $[F]$  to a desired value is traded off against the desire to minimize the resulting disturbance to  $V_{bias}$ , the tradeoff is less severe than in the decentralized case.

In the next section we provide an analytical framework for explaining the improved performance of the multivariable controller.

#### IV. ANALYTIC EXPLANATION OF THE DESIGN

Since Power is the higher bandwidth actuator (cf. Figure 1), we proceed by first closing a Power loop to regulate a linear combination of the two outputs. To determine the appropriate combination of outputs, we apply the properties of Single Input, Two Output (SITO) feedback systems developed in [6].

Denote the first column of  $P$  by  $P_1 = [p_{11} \ p_{21}]^T$  and the first row of  $C$  by  $C_1 = [c_{11} \ c_{12}]$ . With only the Power loop closed, the output sensitivity function is that of the SITO feedback system in Figure 10, and is denoted by

$$S_O^1 = (I + P_1 C_1)^{-1}. \quad (10)$$

It is shown in [6] that the corresponding output complementary sensitivity function,  $T_O^1 = I - S_O^1$ , satisfies

$$\|T_O^1\| = \frac{|T_1|}{\cos \phi_1}, \quad (11)$$

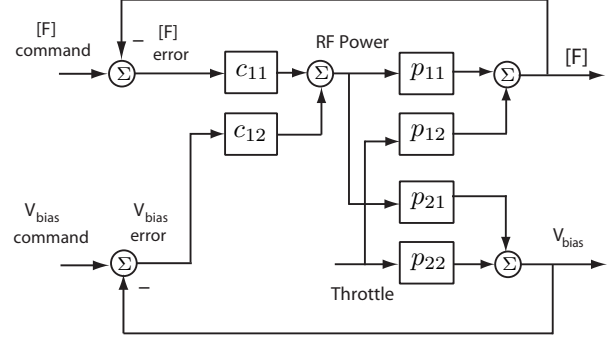


Fig. 10. Power Controls a Combination of  $[F]$  and  $V_{bias}$ .

where  $T_1 = C_1 P_1 / (1 + C_1 P_1)$  and the alignment angle,  $\phi_1$ , is defined by

$$\cos \phi_1 = \frac{|C_1 P_1|}{\|C_1\| \|P_1\|}. \quad (12)$$

If  $\phi_1 = 0^\circ$ , then  $\|T_O^1\|$  has its smallest possible value for a given  $T_1$ . Alternately, if  $\phi_1 \approx 90^\circ$ , then  $T_O$  (and thus  $S_O$ ) will be very large. Moreover, it can be shown that  $\phi_1 \approx 90^\circ$  results in large off-diagonal elements of  $T_O$  and  $S_O$ :

$$|T_{O12}(j\omega)| + |T_{O21}(j\omega)| \geq |T_I(j\omega)| \tan \phi_1(j\omega). \quad (13)$$

For a given  $T_1$ , the off-diagonal elements of  $T_O$  are minimized by choosing  $C_1$  so that  $\phi_1(j\omega) = 0^\circ$ , in which case one may show that the minimum possible interactions are given by

$$|T_{O12}(j\omega)| = |T_{O21}(j\omega)| = \frac{|T_1(j\omega)| |p_{21}(j\omega)/p_{11}(j\omega)|}{1 + |p_{21}(j\omega)/p_{11}(j\omega)|^2}. \quad (14)$$

For the RIE, we have seen that, at low frequencies,  $p_{11}(j\omega) \approx p_{21}(j\omega)$ . Hence choosing  $C_1 = C_{d1} [1 \ 1]$  yields  $\phi_1 \approx 0^\circ$ , and thus the off-diagonal elements of  $T_O$  and  $S_O$  will satisfy (14), yielding  $|T_{O12}| \approx |T_{O21}| \approx 1/2$ .

The preceding analysis supports the results of Section III, wherein we saw that the higher bandwidth Power actuator is used to regulate the average of  $[F]$  and  $V_{bias}$ . We note in passing that a poor choice of controller at those frequencies for which  $p_{11} \approx p_{21}$  would be one of the form  $C_1 = C_{d1} [1 \ -1]$ . At such frequencies the effect of Power on  $[F]$  and  $V_{bias}$  is approximately identical, and feeding back the difference between these two signals would imply that the compensator is attempting to regulate a particular combination of outputs over which it has little control authority. The alignment angle satisfies  $\phi_1 \approx 90^\circ$ , and thus the feedback system would exhibit large interactions and poor robustness.

Let us now determine how the second actuator should be used to obtain a fully multivariable control architecture, as shown in Figure 11. Denote the second column of  $P$  by  $P_2 = [p_{12} \ p_{22}]^T$  and second row of  $C$  by  $C_2 = [c_{21} \ c_{22}]$ . To determine the linear combination of outputs that should be regulated by the second actuator, we first note

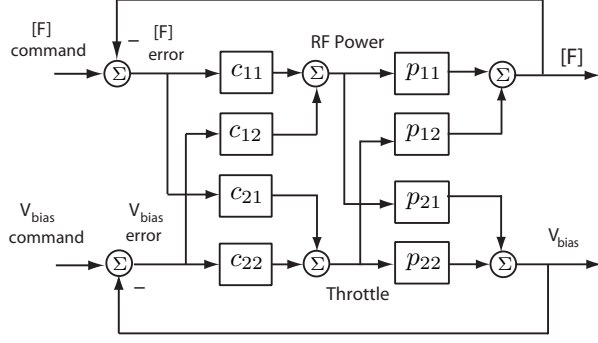


Fig. 11. Fully Multivariable Control.

that the output sensitivity function, which maps commands to tracking errors, has the form

$$S_O = (I + \tilde{P}_2 C_2)^{-1} (I + P_1 C_1)^{-1} \quad (15)$$

$$\tilde{P}_2 \triangleq (I + P_1 C_1)^{-1} P_2, \quad (16)$$

where, in the present case,  $\tilde{P}_2$  is the transfer function from Throttle to the outputs with the Power loop already closed. In the high gain limit, as  $|C_{d1}| \rightarrow \infty$ , we have, from equation (10), that

$$S_O^1 = (I + P_1 C_1)^{-1} \rightarrow I - \frac{P_1 C_1}{C_1 P_1},$$

and thus that

$$\lim_{|C_{d1}| \rightarrow \infty} C_1 \tilde{P}_2 / \|C_1\| = \lim_{|C_{d1}| \rightarrow \infty} C_1 S_O^1 P_2 / \|C_1\| = 0. \quad (17)$$

Since, for the RIE problem, we set  $C_1 = C_{d1} [1 \ 1]$  and let  $|C_{d1}| \rightarrow \infty$ , it follows that  $\tilde{P}_2$  will have a left null-space approximately equal to  $[1 \ 1]$ , and thus the limiting value of  $\tilde{P}_2$  is proportional to  $[1 \ -1]^T$ . Define  $\phi_2$  from  $\cos \phi_2 = |C_2 P_2| / \|C_2\| \|P_2\|$ . Then it follows that choosing  $C_2 = C_{d2} [-1 \ 1]$  will imply that  $\phi_2(j\omega) \approx 0^\circ$  at frequencies for which the gain in the Power loop is large. Hence the second row of the controller will be well aligned with  $\tilde{P}_2$ , the second column of the plant with the first loop closed.

## V. REDESIGN CONTROLLER FOR NEW I/O COMBINATION

In the previous section, we showed that Power and Throttle should be used to track, respectively, the sum and the difference of the outputs  $[F]$  and  $V_{bias}$ . We now use this information to design a multivariable controller directly from first principles, without using the LQ techniques. Since we know the desired controller architecture, this can be done simply by redefining the plant outputs and then applying sequential loop closure. The controller should have the structure  $C = C_d M$ , where

$$C_d = \begin{bmatrix} C_{d1} & 0 \\ 0 & C_{d2} \end{bmatrix} \quad M = \frac{1}{\sqrt{2}} \begin{bmatrix} 1 & 1 \\ -1 & 1 \end{bmatrix}, \quad (18)$$

and  $M$  is used to define new error signals  $(e_1 + e_2)/\sqrt{2}$  and  $(-e_1 + e_2)/\sqrt{2}$ . Then the feedback system has the architecture shown in Figure 12, with output sensitivity function given by

$$S_O = (I + P C_d M)^{-1}. \quad (19)$$

We now convert the problem into one with a decentralized

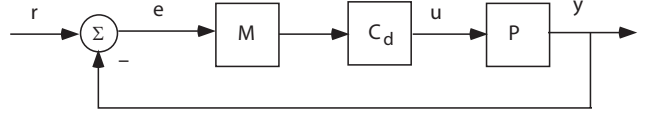


Fig. 12. Control Architecture with Redefined Error Signals.

control architecture by transforming the block diagram in Figure 12 into that of Figure 13. The sensitivity function  $S^M$  describes, in transformed coordinates, the response of the error signal  $e' = M e$  to a command  $r' = M r$ . Hence we can analyze the structure within the dashed box as a decentralized control architecture system with  $C_d$  being the diagonal controller for the transformed plant  $M P$ . Let the elements of the plant,  $P$ , with the ‘‘postcompensator’’  $M$ , be denoted by  $P_{ij}^M$ .

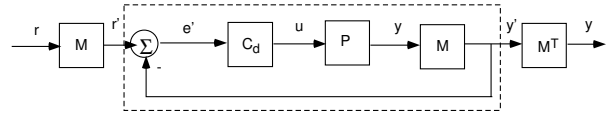


Fig. 13. Transformed Feedback Systems, with Inputs  $(\pm r_1 + r_2)/\sqrt{2}$  and Outputs  $(\pm y_1 + y_2)/\sqrt{2}$ .

It can be shown that  $S_O = M^T S^M M$ , where

$$S^M = (I + M P C_d)^{-1}, \quad (20)$$

and, since  $M$  is orthonormal,  $\|S_O\| = \|S^M\|$ . The ‘‘sensitivity function’’  $S^M$  is used to study tradeoffs arising when a diagonal controller  $C_d$  is designed via sequential loop closure for the plant  $M P$ , whose Bode plots are shown in Figure 14. Note that  $M P$  is much more nearly diagonal at low frequencies than is the original plant. However, there is still interaction at higher frequencies because the original plant no longer satisfies  $p_{11}(j\omega) \approx p_{21}(j\omega)$  at high frequencies. Hence the design tradeoff observed for the previous decentralized control problem is still present, but is not as problematic because the potential interactions lie outside the desired closed loop bandwidth.

The diagonal elements of the compensator,  $C_{d1}$  and  $C_{d2}$ , may be chosen by using the sequential loop closing procedure. When closing the first loop, with the Power actuator, the sensitivity function

$$s_1^M \triangleq 1/(1 + C_{d1} P_{11}^M)$$

describes the ability of the system to track a command of the form  $r_1 = r_2$ . When closing the second loop, the transfer

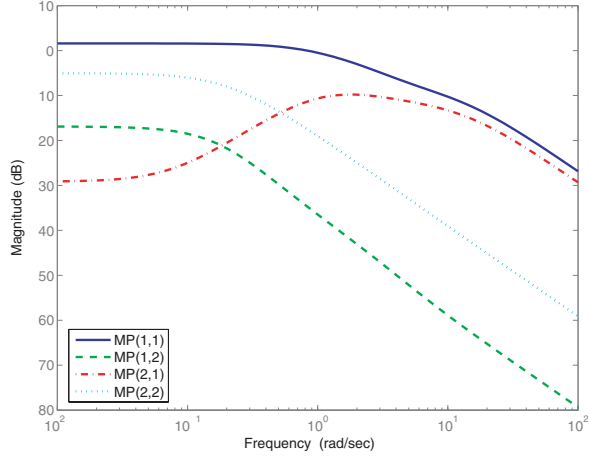


Fig. 14. Bode Plots of the Transformed Plant  $MP$  with Elements  $MP(i, j) = P_{ij}^M$ .

function

$$S_{21}^M = 1/(1 + C_{d2}\tilde{P}_{22}^M)$$

describes the control signal used to track a command of the form  $r_1 = -r_2$ . The off-diagonal element  $S_{21}^M$  describes how the difference in the two outputs,  $y_1 - y_2$ , responds to a command of the form  $r_1 = r_2$ .

It is desirable to make  $s_1^M$  small over a frequency range that is as wide as possible given that the bandwidth in this loop is limited by the presence of measurement noise in the  $[F]$  signal. The bandwidth when closing the second loop must be limited by the need to avoid overshoot in the throttle response. Since the ratio  $P_{21}^M/P_{11}^M$  is small over a low frequency range, the design tradeoff described in Section II is less severe. As a consequence, one can easily design a controller that approximates the performance of the multivariable LQ controller. The step response plots in Figure 15 were obtained using the controller

$$C_{d1} = 0.7(s + 2.1)(s + 1)/(s(s + 5)(s + 1.4))$$

$$C_{d2} = 1.1(s + 0.18)/(s(s + 1)).$$

These responses are comparable to those obtained from the LQ regulator design.

## VI. CONCLUSION AND FUTURE SCOPE

The observation that multivariable controller performs significantly better than a decentralized controller is used as a motivation to analyze the behaviors of the multivariable controller. The concept of using the equivalent controller to reverse engineer a simplified controller from the multivariable controller, implemented on a stable plant, is displayed using the RIE problem. As a justification, the same controller structure is derived using an analytical approach based on [6]. The knowledge of the desired control structure is then used to directly design the controller by using each actuator to track a certain combination of outputs. We note that the use of  $C_{eq}$  for a stable plant obviates

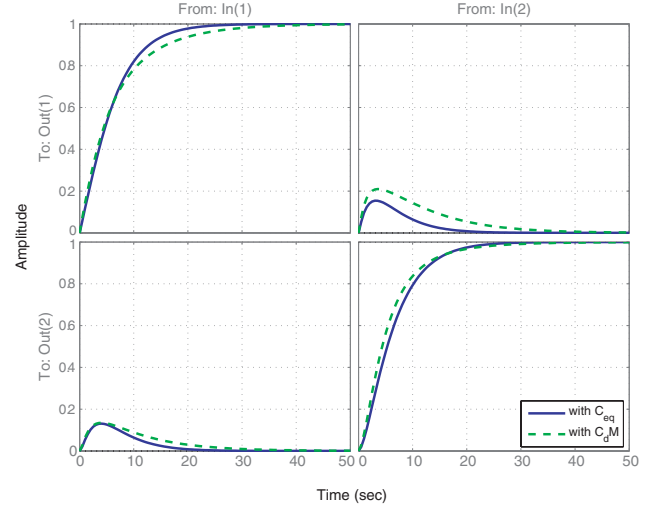


Fig. 15. Step responses in original coordinates that result from sequential loop closure applied to  $MP$ .

the need for an observer design once a state feedback with augmented observers has been obtained. Of course,  $C_{eq}$  will not provide the same response to unmeasurable disturbances. The applications of the equivalent controller analysis to systems with measurable disturbances are found in [8], [9].

## REFERENCES

- [1] J. S. Freudenberg, J. W. Grizzle, and B. A. Rashap. A feedback limitation of decentralized controllers for TITO systems, with application to reactive ion etching. In *Proceedings of the 1994 CDC*, Orlando, FL, 1994.
- [2] M. Elta, et al. Real-time feedback control of reactive ion etching. In *Proceedings of the 1993 SPIE Conference on Microelectronics Manufacturing*, pages 438–451, Monterey, CA, September 1993.
- [3] B. Rashap, J. Freudenberg, and M. Elta. Real-time feedback for sidewall profile control in reactive ion etching. *J. Vac. Sci. Technol. A*, 13(3):1792–1796, May/June 1995.
- [4] B.A. Rashap, et al. Control of semiconductor manufacturing equipment: Real-time feedback control of a reactive ion etcher. *IEEE Transactions on Semiconductor Manufacturing*, 8(3):286–297, August 1995.
- [5] S. Wolf and R.N. Tauber. *Silicon Processing for the VLSI Era: Process Technology*, volume 1. Lattice Press, Sunset Beach, CA, 1986.
- [6] J. Freudenberg and Rick Middleton. Properties of Single Input Two Output Systems, *Int. Journal of Control*, volume 72, no. 16, 1446–1465, 1999.
- [7] A. G. Stefanopoulou and J. S. Freudenberg and J. W. Grizzle. Variable Camshaft Timing Engine Control, *IEEE Transactions on Control Systems Technology*, volume 8, no. 1, 22–34, January 2000.
- [8] A.Y. Karnik, J.H. Buckland and J. S. Freudenberg. Electronic Throttle and Wastegate Control for Turbocharged Gasoline Engines. In *Proceedings of the 2005 ACC*, Portland, OR, 2005.
- [9] C.J. Chiang and A. G. Stefanopoulou. Control of Thermal Ignition in Gasoline Engines. In *Proceedings of the 2005 ACC*, Portland, OR, 2005.